



저작자표시-비영리-변경금지 2.0 대한민국

이용자는 아래의 조건을 따르는 경우에 한하여 자유롭게

- 이 저작물을 복제, 배포, 전송, 전시, 공연 및 방송할 수 있습니다.

다음과 같은 조건을 따라야 합니다:



저작자표시. 귀하는 원저작자를 표시하여야 합니다.



비영리. 귀하는 이 저작물을 영리 목적으로 이용할 수 없습니다.



변경금지. 귀하는 이 저작물을 개작, 변형 또는 가공할 수 없습니다.

- 귀하는, 이 저작물의 재이용이나 배포의 경우, 이 저작물에 적용된 이용허락조건을 명확하게 나타내어야 합니다.
- 저작권자로부터 별도의 허가를 받으면 이러한 조건들은 적용되지 않습니다.

저작권법에 따른 이용자의 권리는 위의 내용에 의하여 영향을 받지 않습니다.

이것은 [이용허락규약\(Legal Code\)](#)을 이해하기 쉽게 요약한 것입니다.

[Disclaimer](#)

**The Differential Effects
of Repetitive Magnetic Stimulation in an *in vitro*
Neuronal Model of Ischemia/reperfusion Injury**

Ji Hyun Kim

The Graduate School
Yonsei University
Department of Medicine

**The Differential Effects
of Repetitive Magnetic Stimulation in an *in vitro*
Neuronal Model of Ischemia/reperfusion Injury**

Directed by Professor Sung Hoon Kim

The Dissertation Submitted to Department of Medicine and the
Graduate School of Yonsei University in partial fulfillment of the
requirements for the degree of Doctor of Philosophy of Medical
Science

Ji Hyun Kim

June 2018

This certifies that the dissertation of Ji Hyun Kim is approved.

Thesis Supervisor : Sung Hoon Kim

Thesis Committee Member : In Deok Kong

Thesis Committee Member : Ji-Yong Lee

Thesis Committee Member : Jang Young Kim

Thesis Committee Member : Sang Baek Koh

The Graduate School

Yonsei University

June 2018

감사의 글

제가 이 자리에 오기까지 바쁘신 중에도 항상 마음 써주시고 지도해 주신 김성훈 교수님께 마음 속 깊이 감사 드립니다. 많이 모자람에도 불구하고 늘 기다려 주시고, 지켜봐 주셔서 여기까지 올 수 있었습니다. 스승님으로서뿐 만 아니라 인생의 큰 조언자가 되어 주시는 교수님께 감사와 존경의 마음을 전하고 싶습니다. 또한 소중한 시간을 내어 지도해 주신 공인덕 교수님, 이지용 교수님, 김장영 교수님, 고상백 교수님께 감사 드립니다.

재활의학교실의 어른으로 늘 든든한 버팀목이 되어 주시는 이영희 교수님, 박정미 교수님께도 이 자리를 빌어 감사의 마음을 전합니다. 교수님들께 배우면서 재활의학과 의사로서의 꿈과 목표를 가질 수 있었고, 바른 의사의 길에 대하여 끊임 없이 고민할 수 있었습니다. 앞으로도 부끄럽지 않은 제자가 되도록 노력하겠습니다.

많이 부족한 딸로 인해 아직도 매일 잠을 설치시며 고생하시는 어머니와, 먼 곳에서 외롭게 지내시는 아버지께도 부끄러운 감사 인사를 전합니다. 오래 고생시켜 드린 만큼 더 큰 기쁨 드릴 수 있도록 노력하겠습니다.

사랑하는 남편과 너무 소중한 두 딸에게 미안함과 사랑을 전합니다.

마지막으로 바쁘다는 핑계로 연락도 자주 드리지 못하지만 저의 남편을 사랑으로 키우시고 저에게 가장 소중한 가족을 꾸릴 수 있도록 해주신 어머니,

아버님께도 감사 드립니다.

2018년 6월

김 지 현 올림

INDEX

FIGURE INDEX	iii
TABLE INDEX	v
ABSTRACT	vi
I. INTRODUCTION	1
II. MATERIALS AND METHODS	4
1. Cell Cultures	4
2. OGD/R and rMS	4
3. Cell Proliferation	7
4. RNA Preparation	7
5. Quantitative Real-Time Reverse Transcription Polymerase Chain Reaction (qRT-PCR)	7
6. Western Blot	8
7. Immunocytochemistry (ICC)	9
8. Terminal dUTP Nick End-Labeling (TUNEL) assay	10
9. Statistical Analysis	10
III. RESULTS	12
1. High-Frequency rMS Increases Cell Proliferation through the Activation of Extracellular Signal-Regulated Kinase (ERK) and AKT Signaling Pathway	

after OGD/R Injury	12
2. High-Frequency rMS Reduces Apoptotic Process after OGD/R Injury	15
3. High-Frequency rMS Increases Ca ²⁺ –CaMKII–CREB Signaling Pathway after OGD/R Injury	18
4. High-Frequency rMS Increases BDNF Expression after OGD/R Injury ..	21
5. High-Frequency rMS Increases Synaptic Plasticity after OGD/R Injury ..	23
IV. DISCUSSION	25
V. CONCLUSION	29
REFERENCES	31
ABSTRAT (IN KOREA)	40

FIGURE INDEX

Figure 1. The experimental timeline of oxygen and glucose deprivation/reoxygenation (OGD/R) exposure and rMS stimulation.	6
Figure 2. High-frequency repetitive magnetic stimulation (rMS) increases proliferation through the extracellular signal-regulated kinase (ERK) and AKT signaling pathway following oxygen and glucose deprivation/reoxygenation (OGD/R) injury.	14
Figure 3. High-frequency repetitive magnetic stimulation (rMS) inhibits apoptosis expression following oxygen and glucose deprivation/reoxygenation (OGD/R) injury.	17
Figure 4. High-frequency repetitive magnetic stimulation (rMS) activates Ca^{2+} -calmodulin-dependent protein kinase II (CaMKII)-cAMP-response element binding protein (CREB) signaling pathway following oxygen and glucose deprivation/reoxygenation (OGD/R) injury.	20
Figure 5. High-frequency repetitive magnetic stimulation increase brain-derived neurotrophic factor (BDNF) expression following oxygen and glucose deprivation/reoxygenation (OGD/R) injury.	22
Figure 6. High-frequency repetitive magnetic stimulation increases synaptic plasticity following oxygen and glucose deprivation/reoxygenation (OGD/R)	

injury.	24
Figure 7. Schematic diagram of the therapeutic mechanisms of repetitive magnetic stimulation (rMS) following ischemia/reperfusion (I/R) injury.	30

TABLE INDEX

Table 1. Primers used for quantitative real-time reverse transcription polymerase chain reaction (qRT-PCR).	8
---	---

ABSTRACT

The Differential effects of repetitive Magnetic stimulation in an In Vitro neuronal Model of ischemia/reperfusion injury

Ji Hyun Kim

Dept. of Medicine

The Graduate School

Yonsei University

Repetitive transcranial magnetic stimulation (rTMS) is a non-invasive therapy that has been implicated in treatment of serious neurological disorders. However, the neurobiological mechanisms underlying the effects of rTMS remain unclear. Therefore, this study examined the differential effects of repetitive magnetic stimulation (rMS) in an in vitro neuronal model of ischemia/reperfusion (I/R) injury, depending on low and high frequency. Neuro-2a cells were differentiated with retinoic acid and established for in vitro neuronal model of I/R injury under a subsequent 3 h of oxygen and glucose deprivation/reoxygenation (OGD/R) condition. After the I/R injury, the differentiated neuronal cells were stimulated with rMS on day 1 and randomly divided into three groups:

OGD/R+sham, OGD/R+low-frequency, and OGD/R+high-frequency groups. High-frequency rMS increases cell proliferation through activation of extracellular signal-regulated kinases and AKT-signaling pathway and inhibits apoptosis in OGD/R-injured cells. Furthermore, high-frequency rMS increases Ca^{2+} -calmodulin-dependent protein kinase II (CaMKII)-cAMP-response element binding protein (CREB) signaling pathway, further leading to alternation of brain-derived neurotrophic factor expression and synaptic plasticity in OGD/R injured cells. These results verified the neurobiological mechanisms of frequency-dependent rMS in I/R injury-treated neuronal cells. These mechanisms will help develop more powerful and credible rTMS stimulation treatment protocols.

Keywords: repetitive magnetic stimulation, high frequency, in vitro neuronal model of ischemia/reperfusion injury

I. INTRODUCTION

Magnetic stimulation produces current flow in the nerve tissue and causes neuronal depolarization (1, 2). Transcranial magnetic stimulation (TMS) generates current flow in the brain without direct contact with the scalp and can be used to assess and control the excitability of certain regions of the brain (1, 3). When induced at a regular frequency, these TMS pulses are called repetitive transcranial magnetic stimulation (rTMS) (4).

rTMS is a non-invasive and less painful method to induce brain stimulation with no significant side effects (1, 5). rTMS is used as a treatment for a wide range of neurologic diseases, such as stroke and movement disorders, psychiatric diseases, and pain syndromes (6).

Several studies have demonstrated that the excitability of the cortex can be differentially modulated by intensity, frequency, and the overall pattern of the rTMS (3). Frequency is an important factor that can control cortical excitability. High-frequency (>3 Hz) stimulation usually has an effect of facilitation while low-frequency (≤ 1 Hz) stimulation has a lowering effect of synaptic efficiency (7–11).

In stroke patients, the motor dysfunction of paretic limb is accompanied by decreased ipsilesional cortical excitability and increased interhemispheric inhibition (IHI) due to the increased contralesional cortical excitability (12). Therefore, rTMS in stroke patients can improve the function of paretic limb by increasing ipsilesional cortical excitability by

applying high frequency rTMS to ipsilesional hemisphere (13–15). There are also several studies that improve the excitability of the ipsilesional cortex via the reduction of the IHI by applying low frequency rTMS to the contralesional hemisphere to improve the function of the paretic limb (16–20).

Furthermore, rTMS treatment is known to affect the regulation of brain plasticity in ischemic stroke patients (21). There are several studies to support neurotrophic factor-mediated brain plasticity as to a mechanism of stroke rehabilitation, and it is known that the expression of brain-derived growth factor (BDNF), which plays an important role in brain plasticity, changes in association with synaptic activity (22). In addition, several in vitro and in vivo studies have shown that rTMS affects the expression of various neurotrophic/growth factors, including BDNF, and neuroblastoma cell proliferation, which has been verified by the various frequencies of rTMS (23–25).

In ischemic stroke, brain injury is caused by ischemia as well as cell damage induced by reperfusion injury (26). Oxygen and glucose deprivation/reoxygenation (OGD/R) is well established in an in vitro model for the study of ischemic/reperfusion (I/R) injury of neurons (27, 28). A previous research confirms that the injury induced by OGD/R can mimic the I/R injury in an in vivo model of ischemic stroke (29).

Although considerable research has been done on the therapeutic use of rTMS for brain ischemic injury, the precise mechanism is still elusive. Therefore, to understand the therapeutic effect and mechanism of rTMS, it is necessary to combine the mechanism

based on brain plasticity. In this study, we aimed to investigate the differential effects of repetitive magnetic stimulation (rMS) depending on frequency in an in vitro neuronal model of I/R injury using OGD/R.

II. MATERIALS AND METHODS

1. Cell Cultures

Neuro-2a (N2a) cells were purchased from American Type Culture Collection biotechnology (ATCC, Manassas, VA, USA).

N2a cells were derived from mouse neuroblastoma, which exhibits properties of neuronal stem cells and could differentiate into neuronal cells when treated with retinoic acid (RA). N2a cells were maintained in growth medium, which were Dulbecco's Modified Eagle Medium (DMEM; Hyclone, Logan, UT, USA) containing 10% fetal bovine serum (FBS; Serum Source International, Charlotte, NC, USA) and 1% Penicillin–Streptomycin solution (Gibco, Rockville, MD, USA), in a humidified 5% CO₂ atmosphere at 37°C. When N2a cells reached 70–80% confluency, the medium was changed into differentiation medium, which contain 2% FBS and 20 μM of RA in DMEM, for 4 days. Differentiated N2a cells were maintained in a humidified atmosphere of 5% CO₂ at 37°C, and the differentiation medium was changed every 2 days.

2. OGD/R and rMS

The following procedures have been adapted from previous studies (29–31). Confluent-differentiated N2a cells were washed three times with phosphate-buffered

saline (PBS) and the differentiation medium was replaced with deoxygenated, glucose-free balanced salt solution (Gibco), and transferred to a hypoxic chamber (O_2 tension 1%) for 3 h. Following OGD, injured cells were replaced with growth medium and stimulated with customized rMS (Bicon-1000Pro, Mcube Technology, Seoul, Korea). The magnetic coil (70-mm diameter) was placed and positioned 1 cm away from the cell culture dish. OGD/R cells were divided into three groups, as the OGD/R+sham group (placing the culture dishes without magnetic stimulation), the OGD/R+low-frequency group (0.5 Hz stimulation, on–off interval of 3 s), and the OGD/R+high-frequency group (10 Hz stimulation, on–off interval of 3 s) for 10 min. After the stimulation, cells were incubated in a humidified atmosphere of 5% CO_2 at 37°C. After 24 h, OGD/R+rMS cells were harvested using 0.25% trypsin-EDTA (Gibco). The experimental schedule is presented in Figure 1. All procedures of the cells were observed under microscope and changed morphology was photographed with a digital imaging system (Eclipse TS100; Nikon USA, Melville, NY, USA) in Figure 2A.

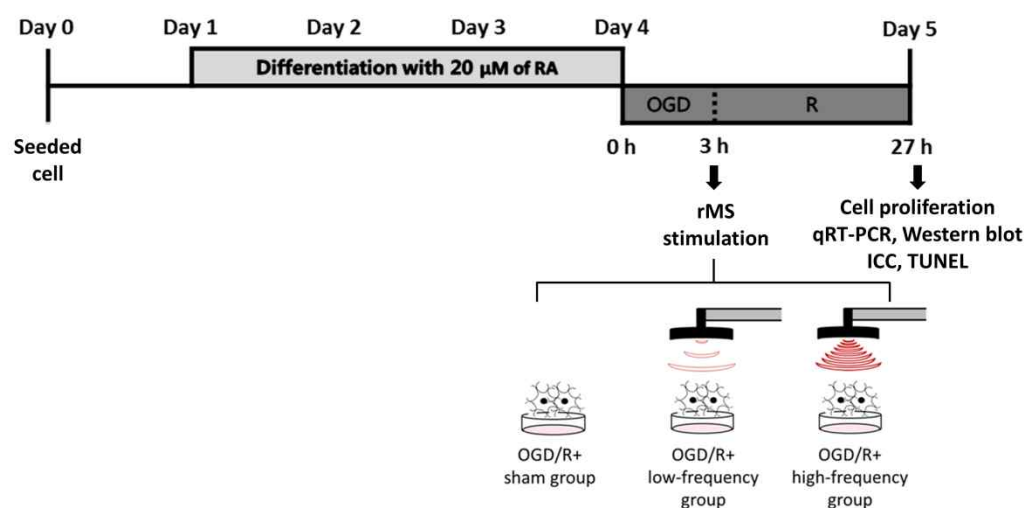


Figure 1. The experimental timeline of oxygen and glucose deprivation/reoxygenation (OGD/R) exposure and RMS stimulation.

On day 0, the equal amount of Neuro-2a (N2a) cells were seeded in growth medium, which contains 10% fetal bovine serum (FBS) and 1% Penicillin–Streptomycin solution. At 70–80% confluency, the growth medium of N2a cells was changed into differentiation medium, which contains 20 μ M of retinoic acid (RA) in Dulbecco’s Modified Eagle Medium (DMEM) for 4 days. After washing three times with PBS, the differentiation medium of N2a cells was changed into deoxygenated, glucose-free balanced salt solution (Gibco) and placed into a hypoxic chamber (O_2 tension 1%) for 3 h. After this OGD injury, the cells were placed with medium and received on–off interval of 3 s stimulation for 10 min. After the stimulation, the cells were incubated in a humidified atmosphere of 5% CO_2 at 37°C. After 24 h, OGD/R+rMS cells were harvested for cell proliferation analysis, qRT-PCR, Western blot, ICC, and TUNEL assay. RA, retinoic acid; OGD/R, oxygen and glucose deprivation/reperfusion; rMS, repetitive magnetic stimulation; qRT-PCR, quantitative real-time reverse transcription polymerase chain reaction; ICC, immunocytochemistry; TUNEL, terminal dUTP nick end-labeling.

3. Cell Proliferation

To analyze the proliferation of the cells, the number of OGD/R+rMS cells was calculated with an advanced detection and accurate measurement (ADAM) automatic cell counter (NanoEnTek Inc., Seoul, South Korea).

4. RNA Preparation

Total RNA was prepared in the whole cell lysates using TRIzol reagent (Invitrogen Life Technologies, Carlsbad, CA, USA) according to the manufacturer's instructions. A nanodrop spectrophotometer (Thermo Fisher Scientific, Waltham, MA, USA) were used to confirm the quality and quantity of extracted RNA.

5. Quantitative Real-Time Reverse Transcription Polymerase Chain Reaction (qRT-PCR)

To examine mRNA expression, qRT-PCR was conducted. ReverTra Ace® qPCR RT Master Mix with gDNA Remover (Toyobo, Osaka, Japan) was used to synthesize cDNA with total RNA. The procedures were according to the manufacturer's instructions. qPCR BIO SyGreen Mix Hi-ROX (PCR BIOSYSTEMS, London, UK) was used to confirm the mRNA expression for genes of interest in a StepOnePlus Real-Time PCR System

(Applied Biosystems, Foster City, CA, USA). Data analysis was performed using the $2^{-\Delta\Delta CT}$ method (32). Primers used for qRT-PCR are described in Table 1.

Table 1. Primers used for qRT-PCR

Gene symbol	Forward primer (5'→3')	Reverse primer (5'→3')
<i>GRIN1</i>	CAG GAT CGT CAG GCA AGA CA	CCA AGC AAC TGA GGG TCC TT
<i>CaMKIIα</i>	TGC TGC TCT TTC TCA CGC TG	TCA ATG GTG GTG TTG GTG CT
<i>CaMKIIδ</i>	TGC ACC TGG TAG GGG ACG AT	GAA TAC AGG GTG GCT TGA TGG GT
<i>BDNF</i>	GGG TCA CAG CGG CAG ATA AA	ATT GCG AGT TCC AGT GCC TT
<i>Synaptophysin</i>	GTG CCA ACA AGA CGG AGA GT	CAC CCG AGG AGG AGT AGT CA
<i>PSD-95</i>	TCC CCA TTT TCT CCC ACA CAC	ACG GCG TGG GGA GTT ATG AT
<i>GAPDH</i>	CAT CAC TGC CAC CCA GAA GAC TG	ATG CCA GTG AGC TTC CCG TTC AG

Grin 1, glutamate receptor ionotropic N-methyl-D-aspartate 1; *CaMKII α* , calcium/calmodulin-dependent protein kinase II alpha; *CaMKII δ* , calcium/calmodulin-dependent protein kinase type II subunit delta; *BDNF*, Brain-derived neurotrophic factor; *PSD-95*, postsynaptic density protein-95; *GAPDH*, Glyceraldehyde-3-phosphate dehydrogenase

6. Western Blot

To confirm the protein expression, whole cell lysates were homogenized and dissolved with radioimmunoprecipitation assay buffer (Thermo Scientific) containing protease and phosphatase inhibitors (Abcam, Cambridge, MA, USA). The BCA™ Protein Assay Kit (Thermo Scientific) was used to quantify the total protein. The samples were denatured and separated by 4–12% Bis-Tris gels in 1×NuPage MES SDS Running Buffer (Invitrogen, Eugene, OR, USA). Proteins were transferred at 4°C onto a polyvinylidene

difluoride membrane (Invitrogen) in NuPage Transfer Buffer (Invitrogen) with 20% (vol/vol) methanol. Membranes were blocked and then incubated overnight at 4°C with the following antibodies: Anti-p-Erk1/2 (1:1,000 dilution, Santa Cruz Biotechnology, Santa Cruz, CA, USA), Anti-t-Erk1/2 (1:1,000 dilution, Santa Cruz Biotechnology), Anti-p-AKT (1:1,000 dilution, Santa Cruz Biotechnology), Anti-t-AKT (1:1,000 dilution, Santa Cruz Biotechnology), Anti-BAX (1: 1,000 dilution, Santa Cruz Biotechnology), Anti-Bcl-2 (1:1,000 dilution, Santa Cruz Biotechnology), Anti-Cleaved-caspase-3 (1:1,000 dilution, Cell Signaling Technology, Danvers, MA, USA), Anti-Pro-caspase-3 (1:1,000 dilution, Santa Cruz Biotechnology), Anti-N-methyl-daspartate receptors1 (NMDAR1; 1: 1,000 dilution, Invitrogen), Anti-CaMKII (1:1,000 dilution, Abcam), Anti-CREB (1:1,000 dilution, Santa Cruz Biotechnology), Anti-p-CREB (1:1,000 dilution, Santa Cruz Biotechnology), Anti-BDNF (1:1,000 dilution, Abcam), and Anti-ACTIN (1:5,000 dilution, Santa Cruz Biotechnology). The next day, blots were washed three times with TBS plus Tween 20 and incubated at room temperature for 1 h with horseradish peroxidase-conjugated secondary antibodies (1:4,000 dilution, Santa Cruz). An enhanced chemiluminescence detection system (Amersham Pharmacia Biotech, Little Chalfont, UK) was used to visualize the protein.

7. Immunocytochemistry (ICC)

To confirm the expression of BDNF, Synaptophysin and postsynaptic density protein-

95 (PSD-95) in differentiated N2a cells were seeded into 0.2% gelatin (Sigma-aldrich, St. Louis, MO, USA) in PBS coated 4-well with OGD/R+rMS stimulation as described above. Cells were stained with Anti-BDNF (1:400 dilution, Abcam), Anti-Synaptophysin (1:400 dilution, Abcam), and Anti-PSD-95 (1:400 dilution, Abcam) and incubated with Alexa Fluor® (1:400, Invitrogen) secondary antibody. Samples were mounted on glass slides with fluorescent mounting medium with 4',6-diamidino-2-phenylindole (DAPI; Vectorshield, Vector Laboratories, Burlingame, CA, USA) for imaging using the Zeiss Axio Imager M2 (Carl Zeiss, Gottingen, Germany) fluorescence microscope.

8. Terminal dUTP Nick End-Labeling (TUNEL) Assay

For analysis of apoptosis, differentiated N2a cells were seeded into gelatin (Sigma-aldrich) coated 4-well. OGD/R and rMS stimulation were performed as described above. Colorimetric TUNEL assay (Promega, Madison, WI, USA) was conducted according to the manufacturer's protocol.

9. Statistical Analysis

All experiments were conducted at least three independent replications. The results were expressed as means \pm SEM. The Statistical Package for Social Sciences version 23.0 was used for statistical analysis. The one-way analysis of variance, followed by

Bonferroni post hoc multi-comparison test was carried out to confirm the statistical results. Statistical differences were considered significant when $p < 0.05$.

III. RESULTS

1. High-Frequency rMS Increases Cell Proliferation through the Activation of Extracellular Signal-Regulated Kinase (ERK) and AKT Signaling Pathway after OGD/R Injury

In the previous study (24), rMS affects cell proliferation in the neuroblastoma cells. Therefore, we evaluated cell proliferation with an ADAM, the automatic cell counting machine, after the stimulation with or without rMS following OGD/R injury.

After 24 h following OGD/R+rMS stimulation, the proliferation rate of the OGD/R+low-frequency group (1.06 ± 0.16) was not significantly different compared to the OGD/R+sham group (Figure 2B). However, in the OGD/R+high-frequency group, proliferation rate was significantly increased compared to the OGD/R+sham group, and the proliferation rate and statistical value were as follows: 3.84 ± 0.64 , $p < 0.001$ (Figure 2B). In the same manner, the proliferation rate of the OGD/R+high-frequency group was significantly increased compared to the OGD/R+low-frequency group ($p < 0.001$) (Figure 2B).

Next, we investigated ERK and AKT pathway, which were known to play an important role in the development of synaptic plasticity and neurotrophic activity (33) as well as the regulation of growth and proliferation (24, 34), by western blot analysis (Figure 2C). The OGD/R+low-frequency group showed the decreased expression of p-ERK and p-AKT

compared to the OGD/ R+sham group and the expression values were as follows: p-ERK/ERK (0.88 ± 0.01 , $p < 0.05$), p-AKT/AKT (0.90 ± 0.01 , $p < 0.01$) (Figure 2D). By contrast, the OGD/R+high-frequency group showed the significantly activated p-ERK and p-AKT expression compared to the OGD/R+sham group, and the expression values were as follows: p-ERK/ERK (1.25 ± 0.02 , $p < 0.001$) and p-AKT/AKT (1.27 ± 0.04 , $p < 0.01$) (Figure 2D). The OGD/R+high-frequency group also showed the significant increased expression of p-ERK and p-AKT compared to the OGD/R+low-frequency group and the expression values were as follows: p-ERK/ERK ($p < 0.001$), p-AKT/AKT ($p < 0.001$) (Figure 2D).

Thus, we suggest that high frequency rMS increases cell proliferation via activation of ERK and AKT signaling pathway following OGD/R injury in differentiated neuronal cells.

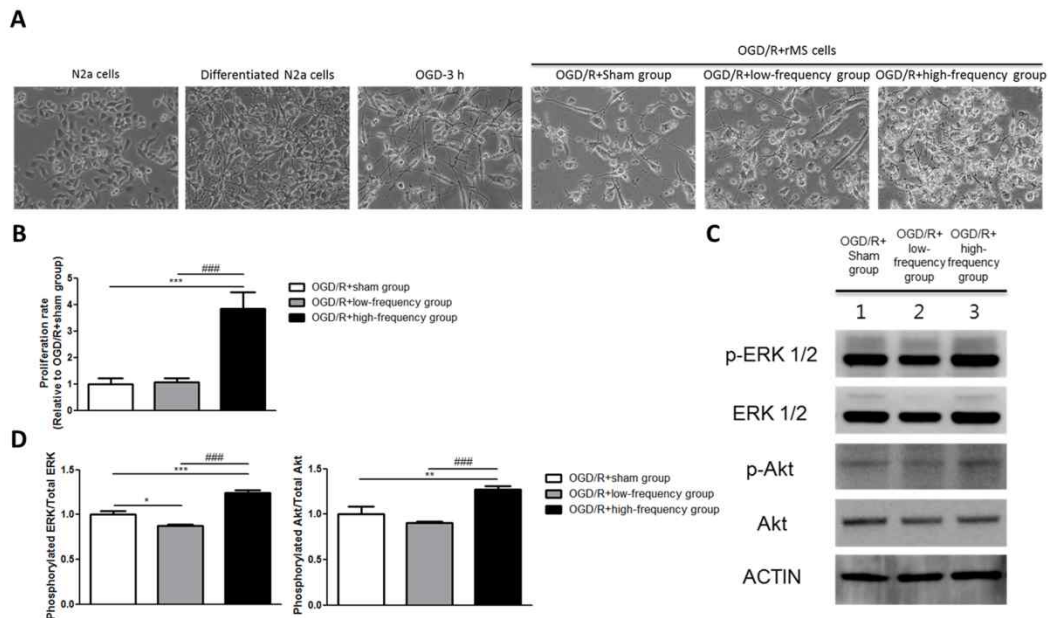


Figure 2. High-frequency repetitive magnetic stimulation (rMS) increases proliferation through the extracellular signal-regulated kinase (ERK) and AKT signaling pathway following oxygen and glucose deprivation/reoxygenation (OGD/R) injury. (A) Changed morphology of the cells was observed under microscope and photographed with a digital imaging system. (B) Bar graphs were shown for the proliferation rate of rMS stimulation following OGD/R injury. The white bars indicate OGD/R+sham group, the gray bars indicate OGD/R+low-frequency group, and the black bars indicate OGD/R+high-frequency group. Proliferation rate was represented as the mean \pm SEM (OGD/R+sham group as control). *** $p < 0.001$ comparison with the OGD/R+sham group. #### $p < 0.001$ comparison with the OGD/R+low-frequency group. (C) Western blot analysis with antibodies against p-ERK, t-ERK, p-AKT, t-AKT, and ACTIN. (D) Comparison of relative expression for p-ERK/ERK and p-AKT/AKT from the OGD/R+rMS-treated group versus the OGD/R+sham group. All results are expressed as means \pm SEM. * $p < 0.05$, ** $p < 0.01$, and *** $p < 0.001$ comparison with the OGD/R+sham group. #### $p < 0.001$ comparison with the OGD/R+low-frequency group.

2. High-Frequency rMS Reduces Apoptotic Process after OGD/R Injury

It has been well demonstrated that neuronal apoptosis is one of the hallmarks of cerebral ischemia/reperfusion (I/R) injury (35). We constructed the OGD/R injury in differentiated neuronal cells to mimic the in vivo cerebral I/R conditions. Apoptotic process was investigated using the protein expressions of apoptosis related proteins, such as Bcl-2-associated X protein (BAX), Bcl-2, Cleaved caspase-3, and Pro-caspase-3 (Figure 3A). As shown in Figures 3A,B, the OGD/R+high-frequency group showed significant decrease in the expression of pro-apoptotic proteins, such as BAX and Cleaved-caspase-3, while showing significant increase in the expression of anti-apoptotic proteins, as Bcl-2 and Pro-caspase-3, compared to the OGD/R+sham group. The expression values were as follows: BAX (0.50 ± 0.08 , $p < 0.001$), Bcl-2 (1.29 ± 0.04 , $p < 0.01$), Cleaved-caspase-3 (0.28 ± 0.04 , $p < 0.001$), and Pro-caspase-3 (1.36 ± 0.03 , $p < 0.001$). In the OGD/R+low-frequency group compared to the OGD/R+sham group, the expression of pro-apoptotic proteins, such as BAX and Cleaved-caspase-3, was increased, while the expression of anti-apoptotic proteins, such as Bcl-2 and Pro-caspase-3, was decreased. The expression values were as follows: BAX (1.32 ± 0.04 , $p < 0.001$), Bcl-2 (0.95 ± 0.03), Cleaved-caspase-3 (1.15 ± 0.02 , $p < 0.05$), and Pro-caspase-3 (1.02 ± 0.05). In the same manner, in the OGD/R+high-frequency group compared to the OGD/R+low-frequency group, the expression of pro-apoptotic proteins was statistically decreased, while the expression of anti-apoptotic proteins was statistically increased. The expression

statistical values were as follows; BAX ($p < 0.001$), Bcl-2 ($p < 0.001$), Cleaved-caspase-3 ($p < 0.001$), and Pro-caspase-3 ($p < 0.01$).

To further investigate the underlying mechanism associated with apoptosis, we used TUNEL assay (Figure 3C). The number of TUNEL-positive nuclei was much observed in the OGD/R+low-frequency group compared to the OGD/R+sham group or the OGD/R+high-frequency group. On the other hand, there were few TUNEL-positive nuclei in the OGD/R+high-frequency group compared to the OGD/R+sham group and the OGD/R+low-frequency group.

These data suggest that high frequency rMS inhibits the progression of apoptosis following OGD/R injury in differentiated neuronal cells.

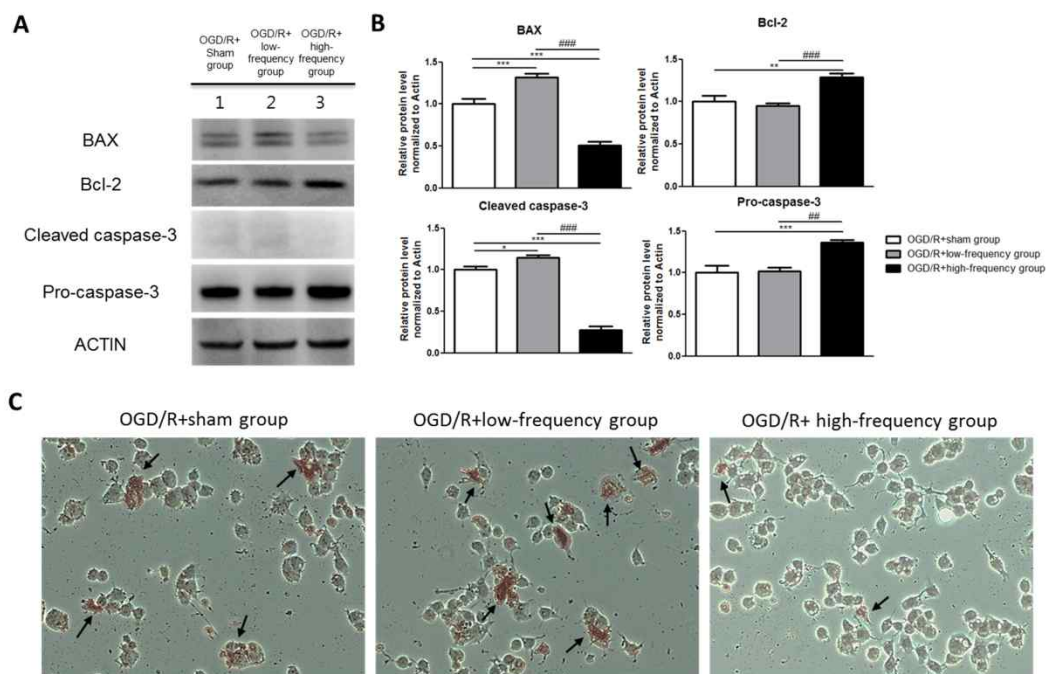


Figure 3. High-frequency repetitive magnetic stimulation (rMS) inhibits apoptosis expression following oxygen and glucose deprivation/reoxygenation (OGD/R) injury. (A) Western blot analysis with antibodies against Bcl-2-associated X protein (BAX), Bcl-2, Cleaved caspase-3, and Pro-caspase-3. (B) Comparison of relative expression apoptosis protein from the OGD/R+rMS treated group versus the OGD/R+sham group. All results are expressed as means \pm SEM. * p < 0.05, ** p < 0.01 and *** p < 0.001 comparison with the OGD/R+sham group. ## p < 0.01 and ### p < 0.001 comparison with the OGD/R+low-frequency group. (C) Detection of apoptosis with terminal dUTP nick end-labeling (TUNEL) assay in the rMS stimulation following OGD/R injury. Black arrow indicates apoptotic nuclei following OGD/R injury in differentiated Neuro-2a (N2a) cells.

3. High-Frequency rMS Increases Ca^{2+} –CaMKII–CREB Signaling Pathway after OGD/R Injury

In our previous study, we confirmed with transcriptome analysis that high frequency rMS can activate Ca^{2+} –CaMKII–CREB signaling pathway, thus increasing the expression of p-CREB and BDNF via the activation of that signaling pathway in the neuronal cells. We further evaluated Ca^{2+} –CaMKII–CREB signaling pathway following OGD/R+rMS stimulation. By qRT-PCR, in the OGD/R+low-frequency group compared to the OGD/R+sham group, the expression of GRIN1, CaMKII α , and CaMKII δ was decreased (Figure 4A). The expression values as follows; GRIN1 (0.71 ± 0.15), CaMKII α (0.72 ± 0.05 , $p < 0.05$), and CaMKII δ (0.36 ± 0.05 , $p < 0.001$). In the OGD/R+high-frequency group, the expression of GRIN1, CaMKII α , and CaMKII δ was significantly increased compared to the OGD/R+sham group (Figure 4A). The expression values were as follows: GRIN1 (1.85 ± 0.20 , $p < 0.01$), CaMKII α (1.27 ± 0.04 , $p < 0.05$), and CaMKII δ (1.28 ± 0.06 , $p < 0.01$). Furthermore, in the OGD/R+high-frequency group compared to the OGD/low-frequency group, the expression of GRIN1, CaMKII α , and CaMKII δ was significantly increased (Figure 4A). The statistical values were as follows: GRIN1 ($p < 0.001$), CaMKII α ($p < 0.001$), and CaMKII δ ($p < 0.001$).

Next, to further evaluate Ca^{2+} –CaMKII–CREB signaling pathway, western blot was conducted (Figure 4B). In the OGD/R+low-frequency group, the expression of N-methyl-d-aspartate receptors1 (NMDAR1), CaMKII, and p-CREB was decreased or no

difference was shown compared to the OGD/R+sham group (Figure 4C). The expression values as follows: NMDAR1 (0.87 ± 0.20), CaMKII (0.86 ± 0.02), and p-CREB (1.19 ± 0.02 , $p < 0.001$). In the OGD/R+high-frequency group, the expression of NMDAR1, CaMKII, and p-CREB was increased compared to the OGD/R+sham group (Figure 4C). The expression values as follows: NMDAR1 (1.25 ± 0.03 , $p < 0.001$), CaMKII (1.31 ± 0.02 , $p < 0.001$), and p-CREB (1.33 ± 0.01 , $p < 0.001$). In the OGD/R+high-frequency group, the expression of NMDAR1, CaMKII, and p-CREB was increased compared to the OGD/R+low-frequency group (Figure 4C). The statistical values were as follows: NMDAR1 ($p < 0.001$), CaMKII ($p < 0.001$), and p-CREB ($p < 0.01$).

Taken together, these data suggest that high frequency of rMS activates Ca^{2+} –CaMKII–CREB signaling pathway following OGD/R injury in differentiated neuronal cells.

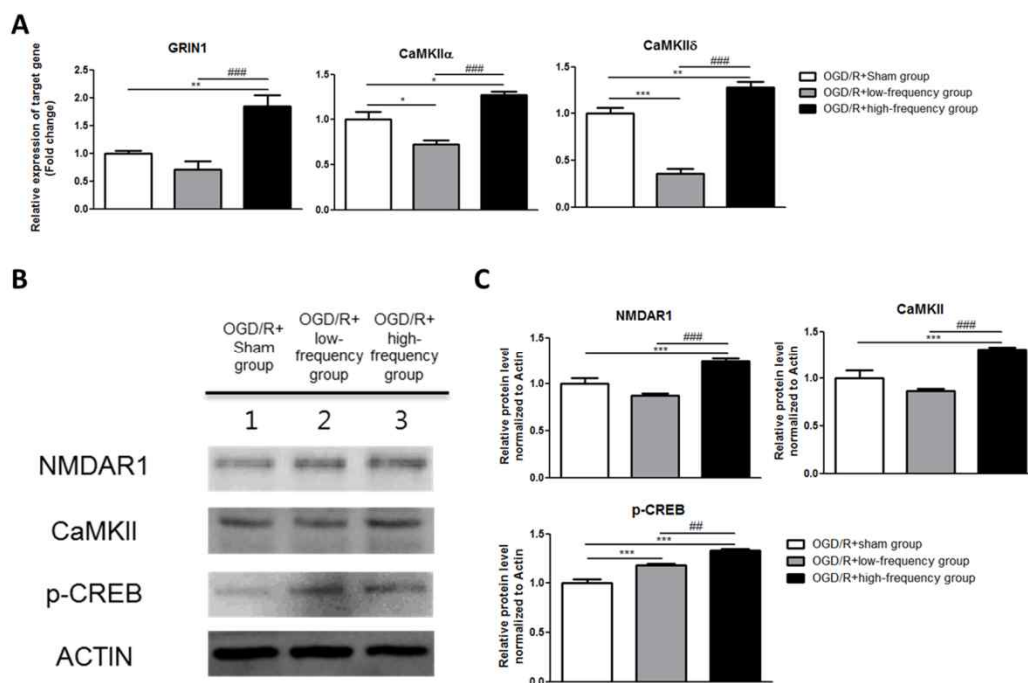


Figure 4. High-frequency repetitive magnetic stimulation (rMS) activates Ca^{2+} -calmodulin-dependent protein kinase II (CaMKII)-cAMP-response element binding protein (CREB) signaling pathway following oxygen and glucose deprivation/reoxygenation (OGD/R) injury. (A) GRIN1, CaMKII α , and CaMKII δ expressions were examined by quantitative real-time reverse transcription polymerase chain reaction. The relative expression of target genes was normalized by the OGD/R+sham group and was calculated using $2^{-\Delta\Delta\text{Ct}}$ method. (B) Western blot analysis was performed using antibodies against N-methyl-d-aspartate receptors1 (NMDAR1), CaMKII, p-CREB, and ACTIN (as control). (C) Comparison of relative expression apoptosis protein from the OGD/R+rMS-treated group versus the OGD/R+sham group. All results are expressed as means \pm SEM. * $p < 0.05$, ** $p < 0.01$, and *** $p < 0.001$ comparison with the OGD/R+sham group. # $p < 0.05$, ## $p < 0.01$, and ### $p < 0.001$ comparison with the OGD/R+low-frequency group.

4. High-Frequency rMS Increases BDNF Expression after OGD/R Injury

In the same manner, we examined the expression of BDNF following OGD/R+rMS stimulation. By qRT-PCR, we found that in the OGD/R+low-frequency group, the expression of BDNF was significantly decreased compared to the OGD/R+sham group, and the expression value was as a follow: BDNF (0.36 ± 0.05 , $p < 0.001$) (Figure 5A). In the OGD/R+high-frequency group, the expression of BDNF was significantly increased compared to the OGD/R+sham group and the expression value was as a follow: BDNF (1.33 ± 0.04 , $p < 0.001$) (Figure 5A). Furthermore, in the OGD/R+high-frequency group compared to the OGD/R+low-frequency group, the expression of BDNF was significantly increased and the statistical value was as follow: BDNF ($p < 0.001$) (Figure 5A).

Then, we further evaluated BDNF expression with ICC analysis (Figure 5B). In the OGD/R+high-frequency group, the protein level of BDNF is significantly higher than the OGD/R+low-frequency or sham group. BDNF expression was significantly decreased, whereas high frequency rMS induces BDNF expression following OGD/R injury in differentiated neuronal cells.

We conclude that high frequency rMS increases BDNF expression via activation of Ca^{2+} -CaMKII-CREB signaling pathway following OGD/R injury in differentiated neuronal cells.

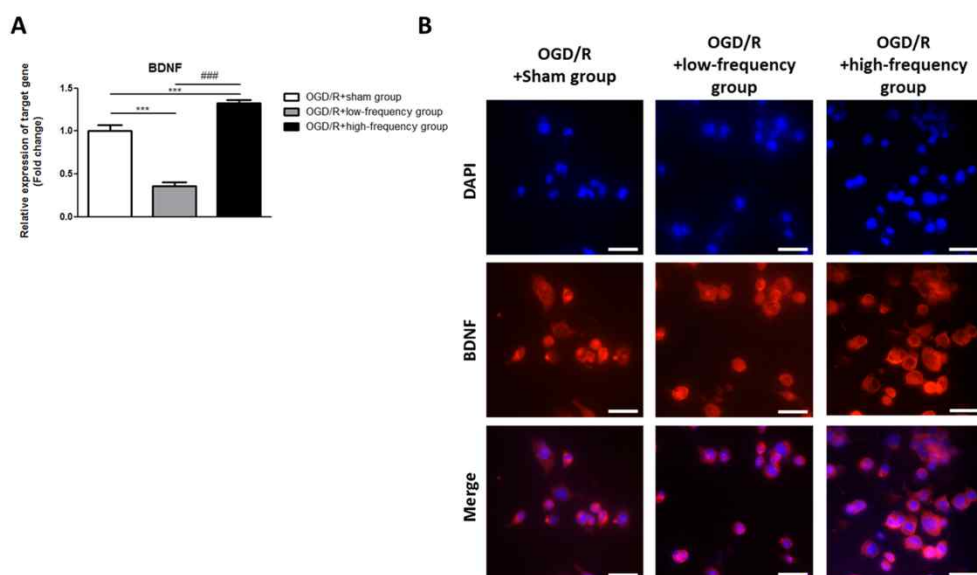


Figure 5. High-frequency repetitive magnetic stimulation increase brain-derived neurotrophic factor (BDNF) expression following oxygen and glucose deprivation/reoxygenation (OGD/R) injury. (A) BDNF mRNA expression was examined by quantitative real-time reverse transcription polymerase chain reaction (qRT-PCR). The relative expression of target gene was normalized by the OGD/R+sham group and was calculated using $2^{-\Delta\Delta C_t}$ method. (B) Immunocytochemistry (ICC) was conducted to evaluate the level of BDNF. Scale bar: 50 μ M, BDNF: Red, 4',6-diamidino-2-phenylindole (DAPI): Blue.

5. High-Frequency rMS Increases Synaptic Plasticity after OGD/R Injury

It is reported that the expression of p-CREB and BDNF is related to the regulation of synaptic plasticity (36, 37). We next assessed synaptic plasticity following OGD/R+rMS stimulation. By qRT-PCR, in the OGD/R+low-frequency group, the expression of synaptophysin, as a presynaptic marker, and PSD-95, as a postsynaptic marker, was significantly decreased compared to the OGD/R+sham group and the expression values were as follows:

Synaptophysin (0.71 ± 0.07) and PSD-95 (0.41 ± 0.05 , $p < 0.01$) (Figure 6A). In the OGD/R+high-frequency group, the expression of synaptophysin and PSD-95 was significantly increased compared to the OGD/R+sham group and the expression values were as follows: Synaptophysin (1.39 ± 0.12 , $p < 0.05$) and PSD-95 (1.38 ± 0.04 , $p < 0.05$) (Figure 6A). In the OGD/R+high-frequency group compared to the OGD/R+low-frequency group, the expression of synaptophysin and PSD-95 was significantly increased and the statistical values were as follows: Synaptophysin ($p < 0.001$) and PSD-95 ($p < 0.001$) (Figure 6A).

Next, we performed ICC analysis to evaluate synaptic plasticity (Figure 6B). In the OGD/R+low-frequency group, the protein level of synaptophysin and PSD-95 was not significantly different compared to the OGD/R+sham group. On the other hand, the protein level of synaptophysin and PSD-95 was significantly increased in the

OGD/R+high-frequency group compared to the OGD/R+low-frequency or sham group.

These data indicated that high frequency rMS increases synaptic plasticity following OGD/R injury in differentiated neuronal cells.

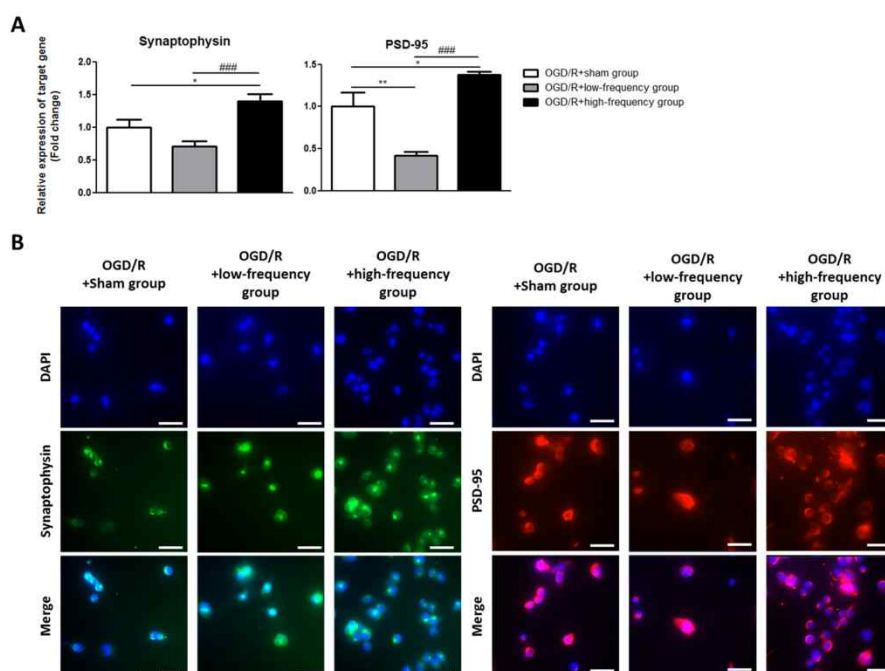


Figure 6. High-frequency repetitive magnetic stimulation increases synaptic plasticity following oxygen and glucose deprivation/reoxygenation (OGD/R) injury. (A) Synaptophysin and postsynaptic density protein-95 (PSD-95) expressions were examined by qRT-PCR. The relative expression of target genes was normalized with respect to the OGD/R+sham group and was calculated using $2^{-\Delta\Delta Ct}$ method. (B) Immunocytochemistry (ICC) was conducted to evaluate the level of synaptophysin and PSD-95. Scale bar: 50 μ M, synaptophysin: Green, PSD-95: Red, 4',6-diamidino-2-phenylindole (DAPI): Blue.

IV. DISCUSSION

Several studies have been conducted to study the effect of rMS on neuronal recovery in the I/R injury model (3, 25, 38, 39). However, the neurobiological mechanism of rMS on the frequency difference in the I/R injury model has not been fully understood. Frequency-dependent stimulation with the same duration has been reported as the primary treatment regime of rMS (38–43). In this study, we developed an I/R injury model using neuronal cells and then applied different frequencies of rMS to it.

It was found that in the high frequency of rMS, cell proliferation was increased, and apoptotic process was decreased compared to the sham or low-frequency rMS following I/R injury. We also verified that the activation of the Ca^{2+} –CaMKII–CREB signaling pathway resulted in increased synaptic plasticity via increasing the expression of BDNF. These results are consistent with the previous studies using neuroblastoma cells, which were transformed neuron-liked cells (23, 24).

In this study, we constructed in vitro I/R injury model to verify accurate therapeutic mechanisms of rMS. When high-frequency rMS was applied to neuronal cells model with I/R injury, activation of the ERK and AKT signaling pathway promoted cell proliferation. These results are consistent with studies using neuroblastoma cells; the effects of rMS-induced cell proliferation were mediated by various growth factors, proliferation-, and survival-associated ERK and AKT (24). ERK and AKT signaling has been known to play an important role in the proliferation and maturation of neural progenitor cells (43, 44) as

well as the regulation of migration of neuroblasts (45).

Next, we verified that high frequency of rMS inhibits the progression of apoptosis in differentiated neuronal cells model with I/R injury. This is in agreement with other in vivo studies. In a study of high-frequency rTMS using a subacute cerebral ischemic rat model, it was suggested that the anti-apoptotic mechanism is the main mechanism of rTMS treatment (39). Another study of the hippocampus area in an ischemic stroke rat model showed that high-frequency rTMS inhibited neuronal apoptosis in ischemic hemispheres (41). In this study, we verified in vitro that high-frequency rMS inhibits the progression of apoptosis, indicating a protective role for the neuronal cells, which have been subjected to I/R injury.

In the brain, BDNF is known to improve neuronal survival, synaptogenesis, angiogenesis, and neurogenesis to regulate neuroplasticity (22, 42, 46, 47). It is also known that rMS affects the expression of BDNF in cultured hippocampal neurons (23). In particular, high frequency of rMS has been shown to increase BDNF expression (24, 25). Our previous study has also shown that the increased expression of BDNF by high-frequency rMS is due to the activation of the Ca^{2+} -CaMKII-CREB signaling pathway.

In this study, using the same method as our previous study, we verified that BDNF expression was increased by the activation of the Ca^{2+} -CaMKII-CREB signaling pathway with high-frequency stimulation in the I/R injury model as well. We also examined that synaptophysin, a presynaptic marker, and PSD-95, a postsynaptic marker,

were both found to increase in high-frequency rMS, thereby improving BDNF-mediated synaptic plasticity. It is thought that, when high-frequency rMS is applied, the various effects due to the increase expression of BDNF may act as a restoring mechanism of the function after I/R injury.

In this study, low-frequency rMS to neuronal cells with I/R injury showed no direct positive effects in cell proliferation, anti-apoptosis, and synaptic plasticity. Previous studies in stroke patients suggested that low-frequency rTMS stimulates the contralesional hemisphere rather than the lesion side, exerting the positive indirect effect and lowering hyper-excitability (48). Therefore, additional follow-up studies will be needed to investigate the molecular mechanism of low frequency rTMS in stroke.

These findings call for further studies on varying degrees of cell regeneration after rMS application, by comparing groups applied with low- and high-frequency rMS after I/R injury and groups neither applied with rMS nor subjected to I/R injury. It is necessary to conduct basic studies to evaluate the functional aspect of cells regenerated by high frequency rMS. In addition, there is a study indicating that the expression of genes involved in cell recovery, such as cell repair and structural remodeling, increases after rTMS in a rat model of cerebral I/R injury (3). Based on this, further studies on cell recovery mechanism after rMS application may be helpful to understand the mechanism of rTMS.

As to the limitation of this study, our data are restricted to the effect of low- and high-

frequency rMS over the same duration, which has been investigated in many previous studies. The different parameters such as the number of magnetic stimuli and duration cannot be disregarded (49–51). Therefore, further prospective studies to evaluate the effect of rMS based on the different durations for both low- and high-frequency rMS are needed.

In this study, we verified the neurobiological mechanism of rMS on I/R injury in neuronal cells, which depends on frequency. These results are valuable as a basic study for understanding the mechanism of rTMS treatment for stroke patients. This mechanism may be useful in developing more robust and reliable rTMS treatment protocols.

V. CONCLUSION

Following I/R injury, neuronal cell death can be induced in an in vitro neuronal model (Figure 7). When high-frequency rMS is treated in the in vitro neuronal model of I/R injury, it can reduce neuronal cell death by increasing cell proliferation and antiapoptosis. Furthermore, it can also increase BDNF expression and synaptic plasticity by activating the Ca^{2+} -CaMKII-CREB pathway. These results demonstrated the combined mechanism of high-frequency rMS in the in vitro neuronal model, and its mechanism could also be applied to other neurological diseases.

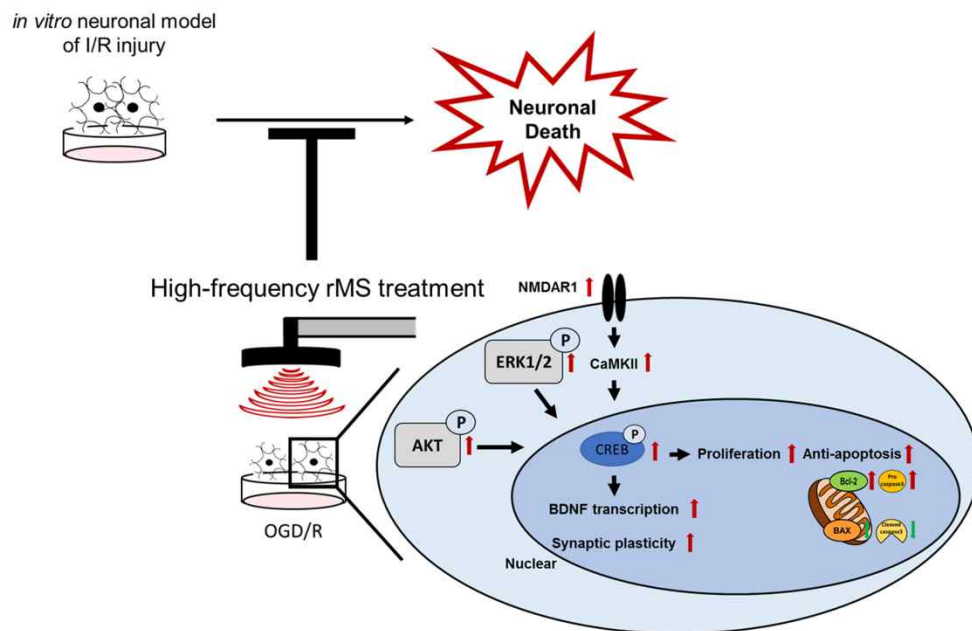


Figure 7. Schematic diagram of the therapeutic mechanisms of repetitive magnetic stimulation (rMS) following ischemia/reperfusion (I/R) injury. High-frequency rMS increases cell proliferation and mediates the protective effects against apoptosis induced by I/R injury. In addition to enhancing the Ca^{2+} -calmodulin-dependent protein kinase II (CaMKII)-cAMP-response element binding protein (CREB) signaling pathway by high-frequency rMS, it also results in activation of brain-derived neurotrophic factor (BDNF) expression and synaptic plasticity in I/R injury.

REFERENCES

1. Barker AT, Jalinous R, Freeston IL. Non-invasive magnetic stimulation of human motor cortex. *Lancet* 1985;1:1106–7.
2. Hallett M. Transcranial magnetic stimulation and the human brain. *Nature* 2000; 406:147–50.
3. Ljubisavljevic MR, Javid A, Oommen J, Parekh K, Nagelkerke N, Shehab S, et al. The effects of different repetitive transcranial magnetic stimulation (rTMS) protocols on cortical gene expression in a rat model of cerebral ischemic reperfusion injury. *PLoS One* 2015;10:e0139892.
4. Fitzgerald PB, Daskalakis ZJ. The effects of repetitive transcranial magnetic stimulation in the treatment of depression. *Expert Rev Med Devices* 2011;8:85–95.
5. Loo CK, Mcfarquhar TF, Mitchell PB. A review of the safety of repetitive transcranial magnetic stimulation as a clinical treatment for depression. *Int J Neuropsychopharmacol* 2008;11:131–47.
6. Lefaucheur JP, Andre-Obadia N, Antal A, Ayache SS, Baeken C, Benninger DH, et al. Evidence-based guidelines on the therapeutic use of repetitive transcranial magnetic stimulation (rTMS). *Clin Neurophysiol* 2014;125:2150–206.
7. Pascual-Leone A, Valls-Sole J, Wassermann EM, Hallett M. Responses to rapid-rate

transcranial magnetic stimulation of the human motor cortex. *Brain* 1994;117(Pt 4):847–58.

8. Chen R, Classen J, Gerloff C, Celnik P, Wassermann EM, Hallett M, et al. Depression of motor cortex excitability by low-frequency transcranial magnetic stimulation. *Neurology* 1997;48:1398–403.

9. Huang YZ, Edwards MJ, Rounis E, Bhatia KP, Rothwell JC. Theta burst stimulation of the human motor cortex. *Neuron* 2005;45:201–6.

10. Houdayer E, Degardin A, Cassim F, Bocquillon P, Derambure P, Devanne H. The effects of low- and high-frequency repetitive TMS on the input/output properties of the human corticospinal pathway. *Exp Brain Res* 2008;187:207–17.

11. Emara TH, Moustafa RR, Elnahas NM, Elganzoury AM, Abdo TA, Mohamed SA, et al. Repetitive transcranial magnetic stimulation at 1Hz and 5Hz produces sustained improvement in motor function and disability after ischaemic stroke. *Eur J Neurol* 2010;17:1203–9.

12. Auriat AM, Neva JL, Peters S, Ferris JK, Boyd LA. A review of transcranial magnetic stimulation and multimodal neuroimaging to characterize post-stroke neuroplasticity. *Front Neurol* 2015;6:226.

13. Khedr EM, Ahmed MA, Fathy N, Rothwell JC. Therapeutic trial of repetitive transcranial magnetic stimulation after acute ischemic stroke. *Neurology* 2005;65:466–8.

14. Kim YH, You SH, Ko MH, Park JW, Lee KH, Jang SH, et al. Repetitive transcranial magnetic stimulation-induced corticomotor excitability and associated motor skill acquisition in chronic stroke. *Stroke* 2006;37:1471–6.
15. Brodie SM, Meehan S, Borich MR, Boyd LA. 5 Hz repetitive transcranial magnetic stimulation over the ipsilesional sensory cortex enhances motor learning after stroke. *Front Hum Neurosci* 2014;8:143.
16. Takeuchi N, Chuma T, Matsuo Y, Watanabe I, Ikoma K. Repetitive transcranial magnetic stimulation of contralesional primary motor cortex improves hand function after stroke. *Stroke* 2005;36:2681–6.
17. Boggio PS, Alonso-Alonso M, Mansur CG, Rigonatti SP, Schlaug G, PascualLeone A, et al. Hand function improvement with low-frequency repetitive transcranial magnetic stimulation of the unaffected hemisphere in a severe case of stroke. *Am J Phys Med Rehabil* 2006;85:927–30.
18. Fregni F, Boggio PS, Valle AC, Rocha RR, Duarte J, Ferreira MJ, et al. A sham-controlled trial of a 5-day course of repetitive transcranial magnetic stimulation of the unaffected hemisphere in stroke patients. *Stroke* 2006;37:2115–22.
19. Meehan SK, Dao E, Lindsell MA, Boyd LA. Continuous theta burst stimulation over the contralesional sensory and motor cortex enhances motor learning post-stroke. *Neurosci Lett* 2011;500:26–30.

20. Tretriluxana J, Kantak S, Tretriluxana S, Wu AD, Fisher BE. Low frequency repetitive transcranial magnetic stimulation to the non-lesioned hemisphere improves paretic arm reach-to-grasp performance after chronic stroke. *Disabil Rehabil Assist Technol* 2013;8:121–4.
21. Dionisio A, Duarte IC, Patricio M, Castelo-Branco M. The use of repetitive transcranial magnetic stimulation for stroke rehabilitation: a systematic review. *J Stroke Cerebrovasc Dis* 2017;27(1):1–31.
22. Johansson BB. Brain plasticity and stroke rehabilitation. The Willis lecture. *Stroke* 2000;31:223–30.
23. Ma J, Zhang Z, Su Y, Kang L, Geng D, Wang Y, et al. Magnetic stimulation modulates structural synaptic plasticity and regulates BDNF-TrkB signal pathway in cultured hippocampal neurons. *Neurochem Int* 2013;62:84–91.
24. Lee JY, Park HJ, Kim JH, Cho BP, Cho SR, Kim SH. Effects of low- and high-frequency repetitive magnetic stimulation on neuronal cell proliferation and growth factor expression: a preliminary report. *Neurosci Lett* 2015;604:167–72.
25. Luo J, Zheng H, Zhang L, Zhang Q, Li L, Pei Z, et al. High-frequency repetitive transcranial magnetic stimulation (rTMS) improves functional recovery by enhancing neurogenesis and activating BDNF/TrkB signaling in ischemic rats. *Int J Mol Sci* 2017; 18:E455.

26. Nour M, Scalzo F, Liebeskind DS. Ischemia-reperfusion injury in stroke. *Interv Neurol* 2013;1:185–99.
27. Abramov AY, Scorziello A, Duchen MR. Three distinct mechanisms generate oxygen free radicals in neurons and contribute to cell death during anoxia and reoxygenation. *J Neurosci* 2007;27:1129–38.
28. Gundimeda U, McNeill TH, Elhiani AA, Schiffman JE, Hinton DR, Gopalakrishna R. Green tea polyphenols precondition against cell death induced by oxygen-glucose deprivation via stimulation of laminin receptor, generation of reactive oxygen species, and activation of protein kinase cepsilon. *J Biol Chem* 2012;287:34694–708.
29. Alluri H, Shaji CA, Davis ML, Tharakan B. Oxygen-glucose deprivation and reoxygenation as an in vitro ischemia-reperfusion injury model for studying blood-brain barrier dysfunction. *J Vis Exp* 2015;99:e52699.
30. Zulueta JJ, Sawhney R, Yu FS, Cote CC, Hassoun PM. Intracellular generation of reactive oxygen species in endothelial cells exposed to anoxiareoxygenation. *Am J Physiol* 1997;272:L897–902.
31. Zhu HY, Wang ZY, Xing YW, Gao YH, Ma T, Lou LX, et al. Baicalin reduces the permeability of the blood-brain barrier during hypoxia in vitro by increasing the expression of tight junction proteins in brain microvascular endothelial cells. *J Ethnopharmacol* 2012;141:714–20.

32. Livak KJ, Schmittgen TD. Analysis of relative gene expression data using realtime quantitative PCR and the $2^{-\Delta\Delta C_T}$ method. *Methods* 2001;25:402–8.
33. Lonze BE, Ginty DD. Function and regulation of CREB family transcription factors in the nervous system. *Neuron* 2002;35:605–23.
34. Adlung L, Kar S, Wagner MC, She B, Chakraborty S, Bao J, et al. Protein abundance of AKT and ERK pathway components governs cell typespecific regulation of proliferation. *Mol Syst Biol* 2017;13:904.
35. Ashkenazi A, Dixit VM. Death receptors: signaling and modulation. *Science* 1998;281:1305–8.
36. Figurov A, Pozzo-Miller LD, Olafsson P, Wang T, Lu B. Regulation of synaptic responses to high-frequency stimulation and LTP by neurotrophins in the hippocampus. *Nature* 1996;381:706–9.
37. Boss V, Roback JD, Young AN, Roback LJ, Weisenhorn DM, Medina-Flores R, et al. Nerve growth factor, but not epidermal growth factor, increases Fra-2 expression and alters Fra-2/JunD binding to AP-1 and CREB binding elements in pheochromocytoma (PC12) cells. *J Neurosci* 2001;21:18–26.
38. Kimbrell TA, Little JT, Dunn RT, Frye MA, Greenberg BD, Wassermann EM, et al. Frequency dependence of antidepressant response to left prefrontal repetitive transcranial magnetic stimulation (rTMS) as a function of baseline cerebral glucose metabolism. *Biol*

Psychiatry 1999;46:1603–13.

39. Chervyakov AV, Chernyavsky AY, Sinitsyn DO, Piradov MA. Possible mechanisms underlying the therapeutic effects of transcranial magnetic stimulation. *Front Hum Neurosci* 2015;9:303.

40. Speer AM, Kimbrell TA, Wassermann EM, D Repella J, Willis MW, Herscovitch P, et al. Opposite effects of high and low frequency rTMS on regional brain activity in depressed patients. *Biol Psychiatry* 2000;48:1133–41.

41. Shaul U, Ben-Shachar D, Karry R, Klein E. Modulation of frequency and duration of repetitive magnetic stimulation affects catecholamine levels and tyrosine hydroxylase activity in human neuroblastoma cells: implication for the antidepressant effect of rTMS. *Int J Neuropsychopharmacol* 2003;6:233–41.

42. Vlachos A, Muller-Dahlhaus F, Rosskopf J, Lenz M, Ziemann U, Deller T. Repetitive magnetic stimulation induces functional and structural plasticity of excitatory postsynapses in mouse organotypic hippocampal slice cultures. *J Neurosci* 2012;32:17514–23.

43. Grehl S, Viola HM, Fuller-Carter PI, Carter KW, Dunlop SA, Hool LC, et al. Cellular and molecular changes to cortical neurons following low intensity repetitive magnetic stimulation at different frequencies. *Brain Stimulat* 2015;8:114–23.

44. Li J, Meng XM, Li RY, Zhang R, Zhang Z, Du YF. Effects of different frequencies of

repetitive transcranial magnetic stimulation on the recovery of upper limb motor dysfunction in patients with subacute cerebral infarction. *Neural Regen Res* 2016; 11:1584–90.

45. Wang L, Zhang ZG, Zhang RL, Gregg SR, Hozeska-Solgot A, Letourneau Y, et al. Matrix metalloproteinase 2 (MMP2) and MMP9 secreted by erythropoietin-activated endothelial cells promote neural progenitor cell migration. *J Neurosci* 2006;26:5996–6003.

46. Park H, Poo MM. Neurotrophin regulation of neural circuit development and function. *Nat Rev Neurosci* 2013;14:7–23.

47. Etcheverrigaray F, Bulteau S, Machon LO, Riche VP, Mauduit N, Leux C, et al. Treating depression with repetitive transcranial magnetic stimulation (rTMS): which repayment of a leading activity in psychiatry? *Rev D Epidemiol Sante Pub* 2017; 65:241–6.

48. Blesneag AV, Slavoaca DF, Popa L, Stan AD, Jemna N, Isai Moldovan F, et al. Low-frequency rTMS in patients with subacute ischemic stroke: clinical evaluation of short and long-term outcomes and neurophysiological assessment of cortical excitability. *J Med Life* 2015;8:378–87.

49. Pascual-Leone A, Houser CM, Reese K, Shotland LI, Grafman J, Sato S, et al. Safety of rapid-rate transcranial magnetic stimulation in normal volunteers.

Electroencephalogr Clin Neurophysiol 1993;89:120–30.

50. Wassermann EM, Grafman J, Berry C, Hollnagel C, Wild K, Clark K, et al. Use and safety of a new repetitive transcranial magnetic stimulator. *Electroencephalogr Clin Neurophysiol* 1996;101:412–7.

51. Mishra BR, Sarkar S, Praharaj SK, Mehta VS, Diwedi S, Nizamie SH. Repetitive transcranial magnetic stimulation in psychiatry. *Ann Indian Acad Neurol* 2011;14:245–50.

Abstract in Korean

허혈/재관류 세포모델에서 다른 주파수에 의한 반복자기자극의 효과

연세대학교 대학원

의학과

김지현

반복경두개자기자극은 비침습적으로 뇌를 자극할 수 있는 방법으로, 통증과 부작용이 적어 여러 가지 심각한 신경계 질환의 치료에 사용되고 있다. 그러나 반복경두개자기자극의 효과를 뒷받침하는 신경 생물학적 기전은 여전히 불분명하다. 따라서 본 연구에서는 허혈/재관류 손상 세포 모델에서 저주파수와 고주파수에 의한 반복자기자극의 효과를 확인하고, 보다 명확한 신경 생물학적 기전을 밝히고자 한다. Neuro-2a 세포를 retinoic acid로 분화시킨 후 3시간 동안 산소와 포도당 결핍/재산소화 조건 하에서 허혈/재관류 손상의 *in vitro* 신경 세포 모델을 구축하였다. 허혈/재관류 손상 후 분화 된 신경 세포는 1일째에 무작위로 반복자기자극을 시행하지 않는 군과, 저주파수 자극을 시행하는 군, 고주파수 자극을 시행하는 군으로 나누었다. 고주파수 반복자기자극은 세포의 신호 조절 키나아제 및 AKT 신호 전달 경로의 활성화를 통해

허혈/재관류 손상 신경세포의 증식을 증가시키고, 사멸을 억제하였다. 또한 고주파 반복자기자극은 Ca^{2+} -CaMKII-CREB 신호 전달 경로를 활성화시켜 허혈/재관류 손상 신경 세포에서 BDNF의 발현 및 시냅스 가소성의 변화를 유도하는 것을 확인할 수 있었다. 이러한 결과는 허혈/재관류 손상 신경 세포에서 주파수의 변화에 따른 반복자기자극 효과의 차이에 대한 신경 생물학적 기전을 명확히 하고, 보다 신뢰할 수 있는 반복경두개자기자극 치료 프로토콜을 개발하는데 도움이 될 것이라 생각한다.

핵심 되는 말 : 반복자기자극, 고주파수, 허혈/재관류 손상 신경 세포 모델